GABA, Glutamate dynamics and BOLD observed during cognitive processing in psychosis patients with hallucinatory traits

Alexander R. Craven[a,b,*],
Gerard Dwyer[a],
Lars Ersland[b],
Katarzyna Kazimierczak[c],
Lin Lilleskare[d],
Ralph Noeske[e],
Lydia Brunvoll Sandøy[a,f]
Erik Johnsen[d,g]
Kenneth Hugdahl[a,d,h]

[a] Department of Biological and Medical Psychology, University of Bergen, Bergen, Norway
[b] Department of Clinical Engineering, Haukeland University Hospital, Bergen, Norway
[c] Institute of Computer Science, Czech Academy of Sciences, Prague, Czechia
[d] Division of Psychiatry, Haukeland University Hospital, Bergen, Norway
[e] GE HealthCare, Berlin, Germany
[f] Department of Physics and Technology, University of Bergen, Bergen, Norway
[g] Department of Clinical Medicine, University of Bergen, Bergen, Norway
[h] Department of Radiology, Haukeland University Hospital, Bergen, Norway

*** Corresponding author:**
Alexander R. Craven (M.Sc.),
Department of Biological and Medical Psychology, University of Bergen,
Jonas Lies vei 91, 5009 Bergen, Norway
Email: alex.craven@uib.no

Word count: 4134 (main text); **200** (abstract)

Abstract:

The perception of a voice in the absence of an external auditory source – an auditory verbal hallucination – is a characteristic symptom of schizophrenia. To better understand this phenomenon requires integration of findings across behavioural, functional, and neurochemical levels. We address this with a locally adapted MEGA-PRESS sequence incorporating interleaved unsuppressed water acquisitions, allowing concurrent assessment of behaviour, blood-oxygenation-level-dependent (BOLD) functional changes, Glutamate+Glutamine (Glx), and GABA, synchronised with a cognitive (flanker) task. We acquired data from the anterior cingulate cortex (ACC) of 51 patients with psychosis (predominantly schizophrenia spectrum disorder) and hallucinations, matched to healthy controls. Consistent with the notion of an excitatory/inhibitory imbalance, we hypothesized differential effects for Glx and GABA between groups, and aberrant dynamics in response to task. Results showed impaired task performance, lower baseline Glx and positive association between Glx and BOLD in patients, contrasting a negative correlation in healthy controls. Task-related increases in Glx were observed in both groups, with no significant difference between groups. No significant effects were observed for GABA. These findings suggest that a putative excitatory/inhibitory imbalance affecting inhibitory control in the ACC is primarily observed as tonic, baseline glutamate differences, rather than GABAergic effects or aberrant dynamics in relation to a task.

Keywords:

GABA; Glutamate; MEGA-PRESS; functional spectroscopy; hallucinations; psychosis

Highlights:

- In-vivo, GABA-edited functional ^{1}H-MRS data were collected from 51 patients with hallucinations and a similar number of matched healthy controls
- Reduced Glutamate+Glutamine (Glx) levels were observed in the patient group.
- BOLD association to baseline Glutamate+Glutamine (Glx) differed between patients and controls
- Robust task-related increases in measured Glx were observed in the Anterior Cingulate Cortex (ACC)
- Task-related changes in measured Glx did not differ between patients and controls

List of Abbreviations

(f)MRI	*(functional) Magnetic Resonance Imaging*
(f)MRS	*(functional) Magnetic Resonance Spectroscopy*
ACC	*Anterior Cingulate Cortex*
AVH	*Auditory Verbal Hallucination*
BAVQ-R	*revised Beliefs About Voices Questionnaire*
BOLD	*blood-oxygenation level dependent*
$CI_{95\%}$	*95% confidence interval*
DDD	*Defined Daily Dose*
DIFF	*GABA-edited difference spectrum*
EPI	*echo-planar imaging*
fGM	*voxel grey matter fraction*
FWHM	*full width at half maximum (measuring spectral linewidth)*
GABA	*γ-aminobutyric acid*
GABA+	*GABA with contribution from underlying co-edited signals*
Glu	*glutamate*
Glx	*Glutamate and Glutamine combined*
HRF	*haemodynamic response function*
ISI	*inter-stimulus interval*
MAD	*Median Absolute Deviation*
MVQ	*MiniVoiceQuestionnaire*
NMDA	*N-methyl-D-aspartic acid*
NAA	*N-acetylaspartate*
P3	*PANSS positive subscale item 3, hallucinatory behaviour*
PANSS	*Positive and Negative Syndrome Scale*
RA	*response accuracy*
RT	*reaction time*
$RT_{slowing}$	*reaction time slowing*
SNR	*signal-to-noise ratio*
SSD	*schizophrenia spectrum disorder*
T_{S-A}	*Time from Stimulus to Acquisition*
$VOI_{(location)}$	*volume of interest (in specified location)*
WREF	*Unsuppressed water-reference spectrum*

1 Introduction

The perception of a voice in the absence of an external auditory source – an auditory verbal hallucination (AVH) – is a characteristic symptom of schizophrenia, manifesting at different "levels of explanation" [1,2]. These range from broad, high-level, macro-scale aspects of cultural and social context, through to clinical symptoms and diagnoses, cognitive factors, and increasingly intricate, mechanistic aspects of integrated neural systems and networks, individual synapses and neurotransmitters forming a part of those systems, and the molecular processes occurring therein. While observations at all levels have been informative in guiding targets for treatment and for further research, these when considered in isolation have not yielded a comprehensive explanation of the complex, multi-faceted phenomenon. Indeed, without effective vertical integration to harmonise findings across levels there is a risk that the theories and models under investigation become dissociated from the very phenomena which they attempt to explain[1].

Amongst current theories aiming to explain the phenomenology of patients "hearing voices" is a putative breakdown of the dynamic interplay between bottom-up (excitatory, perceptual) and top-down (inhibitory control) cognitive processes, perhaps reflected in the dynamic interaction of excitatory and inhibitory neurotransmitters[3]: glutamate (Glu) and γ-aminobutyric acid (GABA) respectively. While there are published imaging and static spectroscopy findings to support this model[2,4], there is currently limited data to bridge clinical and imaging findings with neurotransmitter dynamics at the receptor level, due in part to the challenges associated with reliably measuring these neurotransmitters in a dynamic (functional) setting.

Acquisition and reliable analysis of functional Magnetic Resonance Spectroscopy (fMRS) data is challenging for two reasons: firstly, the metabolite signals of interest are

several orders of magnitude weaker than the water signal which forms the basis of blood-oxygenation level dependent (BOLD) functional Magnetic Resonance Imaging (fMRI) measurement, leading to a substantial trade-off against spatial and temporal resolution. Furthermore, BOLD-related changes in signal relaxation and local shim quality have a direct impact on spectral line-shape which may affect the quantification of certain metabolites. While this represents a potential confound for metabolite quantification[5], it also provides an opportunity for simultaneously assessing task-induced BOLD dynamics from unsuppressed water data obtained during the MRS acquisition[6,7]. Extending the approach of Apšvalka et al [8] to a GABA-editing (MEGA-PRESS) context[9,10], we previously demonstrated a technique for simultaneously obtaining time-resolved, GABA-edited, MRS data and an indication of local BOLD response[11], incorporating unsuppressed water reference signals at a regular interval within the edited acquisition scheme. The GABA-editing technique yields estimates for GABA with some contribution from underlying co-edited signals (GABA+), and estimates for Glutamate and Glutamine combined (Glx). The present study applies the same acquisition and analysis techniques (and a matched subset of the same healthy controls) in a case-control context with psychosis patients, predominantly with a diagnosed schizophrenia spectrum disorder (SSD).

Consistent with the notion of an excitatory/inhibitory imbalance, we hypothesize differential effects for Glx and GABA between healthy controls and patients, and aberrant dynamics in one or both in relation to a cognitive task. Furthermore, based on the findings of Falkenberg et al [12], we anticipate positive correlation between BOLD-fMRI activation and baseline Glx in the patient group, with decreased Glx levels associated with impaired executive control functioning in that group. We further anticipate a negative correlation between BOLD-fMRI activation and baseline Glx in the healthy controls.

2 Methods

2.1 In-vivo data collection

2.1.1 Subject recruitment and demographics

The study included 54 psychiatric patients experiencing mild to severe AVH. Patients were recruited through health-care personnel in the Vestland County Health Care System (Helse Vest regional helseforetak). The recruitment was primarily from the Sandviken Psychiatric Clinic, Haukeland University Hospital in Bergen, Norway, with a few patients recruited from other counties. Patients had different psychiatric diagnoses, predominantly on the schizophrenia spectrum (see Supplementary Table 1 for ICD-10 diagnoses[13,14]). Prior to inclusion (and no more than 7 days before MR scanning), patients underwent a Positive and Negative Syndrome Scale (PANSS)[15] interview. Only patients exhibiting hallucinatory behaviour according to a PANSS positive subscale item 3 (P3) score of 3 or higher were recruited to the study. Subsequently, the project nurse administered the revised Beliefs About Voices Questionnaire (BAVQ-R)[16] and the MiniVoiceQuestionnaire (MVQ)[17]. Of the initially scanned participants, three patients were excluded due to technical issues, giving a total of 51 patients (19 female, 20 male, 2 transgender assigned female at birth), mean age 31.8 years (SD 9.3) with a mean PANSS P3 score of 4.6 (SD 0.8). Most patients used second-generation antipsychotics, with prescribed maximum dosage around 1.36 (SD 1.47) times the Defined Daily Dose (DDD)[18]; further detail in Supplementary Figure 1.

An equal number of healthy controls were included, matched on age (± 4 years): mean age 31.5 years (SD 9.1); two transgender patients were matched according to the sex they were assigned at birth. Healthy controls were drawn from a larger cohort which has been analysed previously to demonstrate efficacy of the applied methods [11].

All potential subjects were screened for implanted medical devices and history of major head injuries; controls were additionally screened for substance abuse, and for neurological or medical illnesses. All subjects provided written informed consent prior to participation and were free to withdraw at any time without consequence. Participants received compensation in the form of cash or a gift card. The study was approved by the Regional Committee for Medical Research Ethics in Western Norway (REK Vest # 2016/800).

2.1.2 MR scanning protocol

MR data were acquired on a 3.0 T GE Discovery^{TM} MR750 scanner (GE HealthCare, Chicago, IL), with an 8-channel head coil. The protocol included a high-resolution T1-weighted structural acquisition: fast spoiled gradient (FSPGR) sequence with 188 sagittal slices of 256x256 isometric 1 mm voxels, 12 degree flip angle and TE/TR approximately 2.95/6.8 ms respectively. GABA-edited MRS data were acquired with a modified MEGA-PRESS sequence (TE=68 ms, TR=1500 ms, 15ms editing pulses at 1.9/7.46 ppm for edit-ON/-OFF respectively, simple 2-step phase cycle to minimize periodic confounds, 700 transients total), from a 22x36x23 mm (18.2 mL) voxel placed medially in the Anterior Cingulate Cortex (ACC). This voxel was centred on an imaginary line projected through the forward part of the pons, parallel with the brain stem as illustrated in Figure 1. The standard GE HealthCare MEGA-PRESS implementation had been modified to send per-TR trigger pulses for task synchronisation, and to periodically disable CHESS water suppression (every third transient) to allow acquisition of a water-unsuppressed reference signal interleaved within the regular GABA-editing sequence [11]. A summary of key sequence and hardware parameters is presented in an MRSinMRS[19] checklist, Supplementary Table 2.

Finally, BOLD fMRI data were collected with an echo-planar imaging (EPI) sequence: TE=30 ms, TR=2500 ms, 90 degree flip angle, interleaved acquisition of 36 slices of 128 x

128 voxels (1.72x1.72 mm), 3.0 mm slice thickness with 0.5 mm gap (3.5 mm slice spacing); 240 volumes for a total acquisition time of 600 s. Two patients elected to end scanning before completion of the BOLD fMRI task, and are therefore excluded only from analyses relating to that sequence.

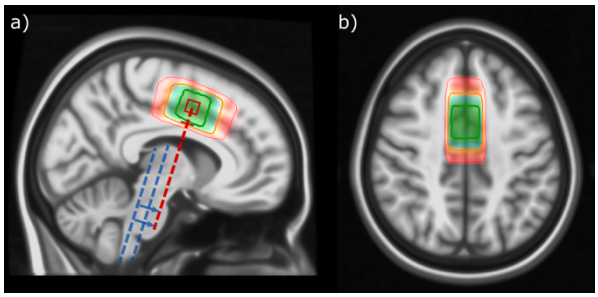

Figure 1: Placement of the fMRS voxel across all subjects, mapped to standard space. Shading (red-blue-green) and corresponding contours indicate [5,50,95]-percentile coverage of the achieved placement across subjects. Dashed lines in (a) illustrate landmarks used for voxel positioning: medial ACC, centred on an imaginary line through the forward part of the pons (red), parallel with the brain stem (indicated in blue). Adapted from Craven et al, 2023[11], updated to reflect the present sample.

2.1.3 Functional paradigm: Eriksen Flanker task

During both the GABA-edited fMRS and the BOLD fMRI acquisitions, subjects performed a cognitive task based on the Eriksen Flanker task[20]. In each trial, a set of five arrows is presented; the task is to indicate the direction of the central "target" arrow. The four surrounding "flankers" may match the target for a "congruent" trial (for example, " > > > > > " or " < < < < < "), or they may be in the opposite direction for a cognitively more demanding "incongruent" trial (" < < > < < " or " > > < > > "). The paradigm was implemented in E-Prime 2.0 SP1 [2.0.10.353: Psychology Software Tools Inc., Pittsburgh, PA, https://pstnet.com/], with timing synchronised to the scanner via an NNL SyncBox [NordicNeuroLab AS (NNL), Bergen, Norway, http://nordicneurolab.com/, note declaration of interest]. Stimuli were presented through goggles (NNL) in light grey on a black background, with a small font to remain near the parafoveal field of view[21]. Subjects

responded using handheld response grips (NNL), pressing with the index finger on the corresponding hand. Subjects were presented instructions in Norwegian or English according to preference, and were shown sample stimuli before entering the scanner, and again immediately before the task.

The task was implemented in a block-event design, beginning with a 60-second task-OFF block then alternating 30-second task-ON and 60-second task-OFF blocks, for a total of 11/6 task-ON blocks for the fMRS/fMRI acquisitions respectively. Within each task-ON block, one trail was presented per TR giving an average inter-stimulus interval (ISI) of 1500 ms and a total of 220/120 trials for fMRS/fMRI respectively. A randomly selected 40% of trials were incongruent. Trial onset timing was jittered randomly with respect to the fixed TR, such that stimuli were presented in the range $T_{S\text{-}A}$ = 100-350 ms before the excitation pulse, spanning much of the early response suggested by prior fMRS studies[8,22]. Stimuli were presented for 350 ms, with a nominal 800 ms response window.

2.2 fMRS data processing and quantification

Functional MEGA-PRESS data were processed with a modified pipeline based around core functionality from Gannet version 3.1 [23]. After spectral registration[24,25], individual transients were processed using a linear model to separate variance of interest from nuisance factors (variance associated with phase cycling and inferred subject motion), as detailed in a previous work [11,26]. Spectra were modelled according to achieved interval between stimulus and acquisition ($T_{S\text{-}A}$). Five bins were defined, with edges at [100, 183, 267, 350] ms, open at either end, lower limits inclusive; the inner three bins evenly cover the nominated 100-350 ms $T_{S\text{-}A}$ range. This resulted in approximately 48 task-ON metabolite transients per bin (with some individual variation), and 320 task-OFF metabolite transients. Line-shape matching was performed using a reference deconvolution approach[26–29].

Extracted GABA-edited difference spectra (DIFF) were evaluated against three rejection criteria, applied in series: full width at half maximum (FWHM) linewidth of fitted GABA+ or inverted N-acetylaspartate (NAA) peaks exceeding 30 Hz or 12 Hz respectively, extraordinarily low signal-to-noise ratio (SNR) (below 20 for the fitted NAA peak), and extreme outliers, where GABA+ or Glx estimates differed from the median by more than five times the Median Absolute Deviation (MAD) for spectra surviving the first two criteria.

Unsuppressed water-reference spectra (WREF) were fit with a pseudo-Voigt function on a linear baseline, with Voigt linewidth filtered for outliers and discontinuities and modelled against the expected BOLD response (event impulses convolved with a dual-gamma haemodynamic response function (HRF) model), with covariate components as for the metabolite spectrum model. The resultant BOLD model coefficient estimates the overall change in water linewidth ($\Delta FWHM_{water}$) reflecting the strength of the individual's BOLD response within the fMRS-localised region[11]. This value will be denoted BOLD-fMRS.

2.3 fMRI data processing

fMRI block analysis was performed using FEAT (FMRI Expert Analysis Tool version 6.00, part of FSL) [30–37], with a standard pipeline described fully in our previous work[11]. For the present study, a per-subject volume of interest (VOI) is defined from the individually prescribed fMRS voxel geometry in the ACC ($VOI_{fMRS,ACC}$), with the median Z-score (without thresholding) across $VOI_{fMRS,ACC}$ taken as a measure of the strength of the BOLD response across that volume. This value will be denoted BOLD-fMRI.

2.4 Numerical and Statistical Analysis

Behavioural outcomes were assessed with the Wilcoxon Signed Rank test for related samples (between session/stimulus, within subject), and the Mann-Whitney U-test for unrelated samples (patient vs control), motivated by unequal variance and high skew in some

parameters. Correlation of BOLD estimates by the two methods (BOLD-fMRI, BOLD-fMRS) was assessed using the skipped Spearman method[38,39] for resilience to bivariate outliers. Outcomes from hypothesis testing and correlational tests are adjusted for multiple comparisons within sub-analysis, using the Holm-Bonferroni approach; adjusted p-values are denoted p_{holm}, with a corrected significance threshold defined as $p_{holm}<0.05$.

Least-squares linear modelling was used to assess associations between baseline metabolite estimates, BOLD signal strength and interactions with patient and control groups, with voxel grey matter fraction (fGM) as a covariate (ie, `Glx ~ C(group)*BOLD + fGM`). Outlier observations having disproportionate influence on the model (according to the studentized difference in fits[40] thresholded at $2\sqrt{(k/n)}$) were dropped. Model suitability was verified using the Jarque-Bera test of normality[41], and White's Lagrange Multiplier and Two-Moment Specification tests[42] for heteroscedasticity and correct specification.

A series of exploratory correlational tests were performed between symptom scores (PANSS: P3, total positive and total negative subscale scores) and baseline metabolite concentrations (Glx, GABA+), task-elicited change in metabolite levels (ie, $\Delta Glx = Glx_{task\text{-}ON} - Glx_{task\text{-}OFF}$ and $\Delta GABA = GABA_{task\text{-}ON} - GABA_{task\text{-}OFF}$), BOLD response, and task performance metrics (response accuracy (RA)/reaction time (RT), reaction time slowing ($RT_{slowing}$)), using the skipped Spearman method.

Finally, a linear mixed-effects model was constructed for metabolite estimate in relation to group (patient, control), task status (task-OFF, task-ON), with grey matter fraction as a covariate and subject as the grouping variable (ie, `Glx ~ C(group)*C(task_state) + fGM`), filtering observations with strong residuals (deviating from median residual by more than 2.5 times the MAD).

Statistical testing was performed in Python (v3.9.17) with statsmodels [43] (v0.13.5), pingouin [44] (v0.5.2), SciPy [45] (v1.9.3), pandas [46] (v1.5.2) and NumPy [47] (v1.23.5) libraries; subsequent visualisation was built on tools from matplotlib [48] (v3.3.4), seaborn [49] (v0.11.2) and statannotations [50] (v0.5).

3 Results

3.1 Behavioural Outcomes

Behavioural outcomes from the Flanker task are summarised in Figure 2 and Supplementary Table 3. Task performance in terms of reaction time (RT), response accuracy (RA) and RA/RT was significantly degraded (p_{holm}<0.001) between congruent and incongruent trials, assessed across all subjects. Improved RA and RA/RT were observed between the fMRS and subsequent fMRI task, both strongly significant for incongruent stimuli (p_{holm}<0.001). Patients showed significantly lower RA and RA/RT than the healthy controls (p_{holm}<0.001).

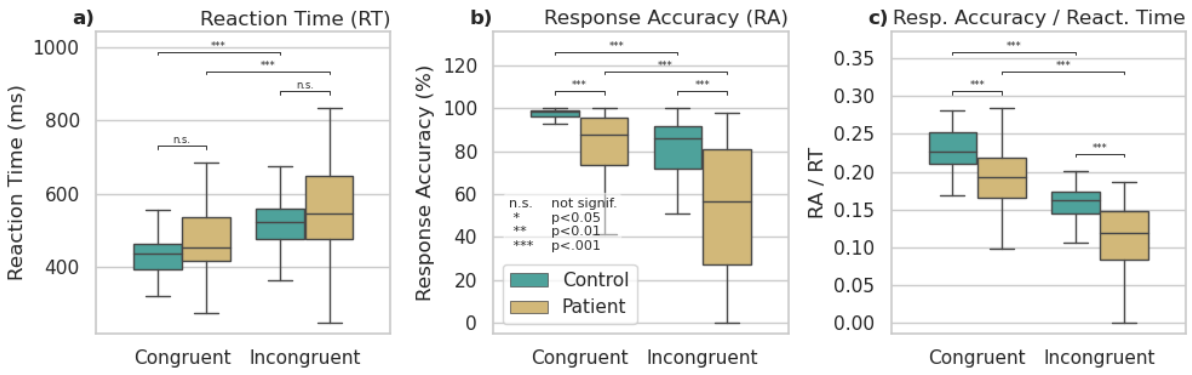

*Figure 2 Outcomes from the behavioural task (fMRS and fMRI sessions pooled), showing significant increase in reaction time (a) and reduction in response accuracy (b, c) for incongruent conditions, and significantly degraded response accuracy for patients. Significant differences indicated with *** p_{holm}<0.001, ** p_{holm}<0.01, * p_{holm}<0.05, n.s. not significant*

3.2 Functional Outcomes

3.2.1 BOLD assessment by fMRI and fMRS

Correlation between the strength of the BOLD response as assessed with fMRS and fMRI methods within the individually prescribed $VOI_{fMRS,ACC}$ was significant for healthy controls (r=0.35, 95% confidence interval ($CI_{95\%}$) [0.07,0.57], p=0.014), but unreliable for the patient group (r=-0.08, $CI_{95\%}$ [-0.353,0.212], p>0.5), combining to a weak correlation across the entire dataset (r=0.16, $CI_{95\%}$ [-0.04,0.346], n.s.). Correlation by group is shown in Figure 3; note generally weaker BOLD-fMRI response and greater variance in the BOLD-fMRS estimate amongst patients.

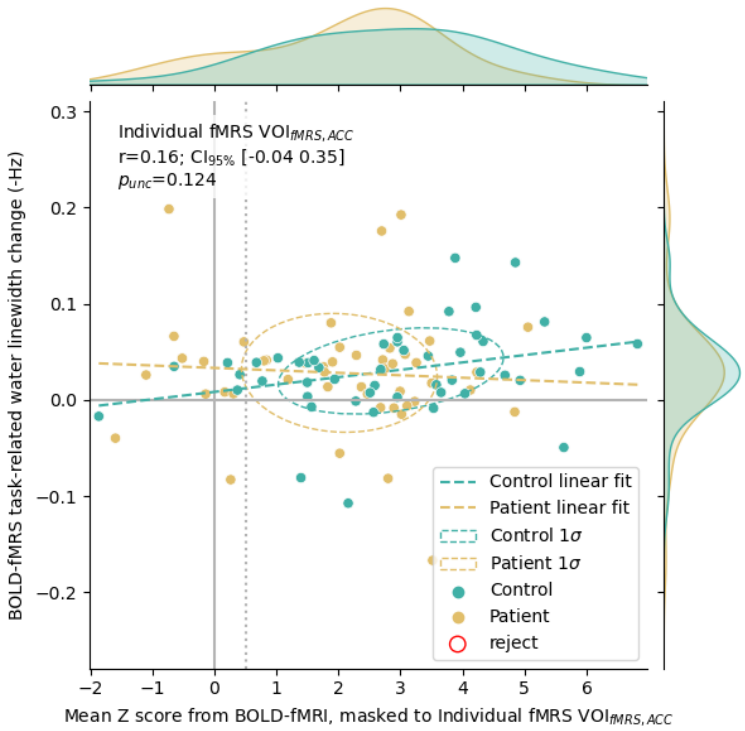

Figure 3 Relation of BOLD assessed by BOLD-fMRS linewidth changes ($\Delta FWHM_{water}$) to mean Z score observed from the BOLD-fMRI data, regionally masked to the individual fMRS voxel ($VOI_{fMRS,ACC}$)), showing significant correlation specific to healthy controls.

3.2.2 Baseline and Functional MRS

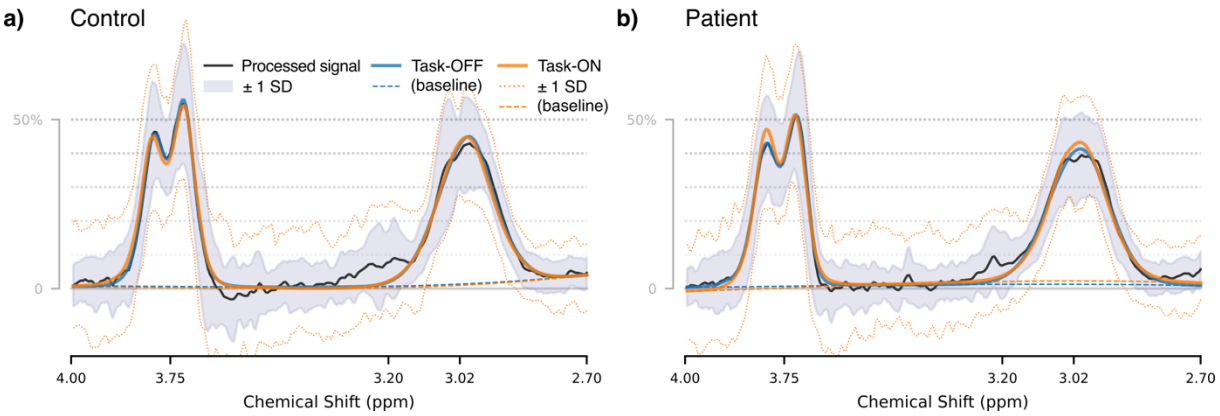

Figure 4 Group mean spectra and model fit, separated by task condition

Mean measured spectra for each group and condition are presented in Figure 4, with corresponding quality metrics in Supplementary Table 4. Association with BOLD-fMRI is shown in Figure 5. The linear model for baseline metabolite concentration with factors for the interaction between group and measured BOLD strength (BOLD-fMRI) and grey matter fraction showed significant effects of group for Glx (-2.3603 i.u., $CI_{95\%}$ [-3.680, -1.040], $p<0.001$), a main effect for BOLD-fMRI (b=-0.394, $CI_{95\%}$ [-0.686,-0.102], $p<0.01$) and an interaction between group and BOLD-fMRI (b=0.586, $CI_{95\%}$ [0.113, 1.059], p=0.016). This indicated lower baseline Glx in patients and differential association between BOLD and baseline Glx amongst healthy controls (negative association) and patients (positive association). All other factors were non-significant. Substituting BOLD-fMRS as the independent variable yielded weaker outcomes (p=0.054 for the group effect, p=0.094 for the main effect of BOLD-fMRS). Similar analyses for GABA+ yielded no significant results. Detailed model output is presented in the Supplementary Material, sections C.1 and C.2 for Glx and GABA+ respectively.

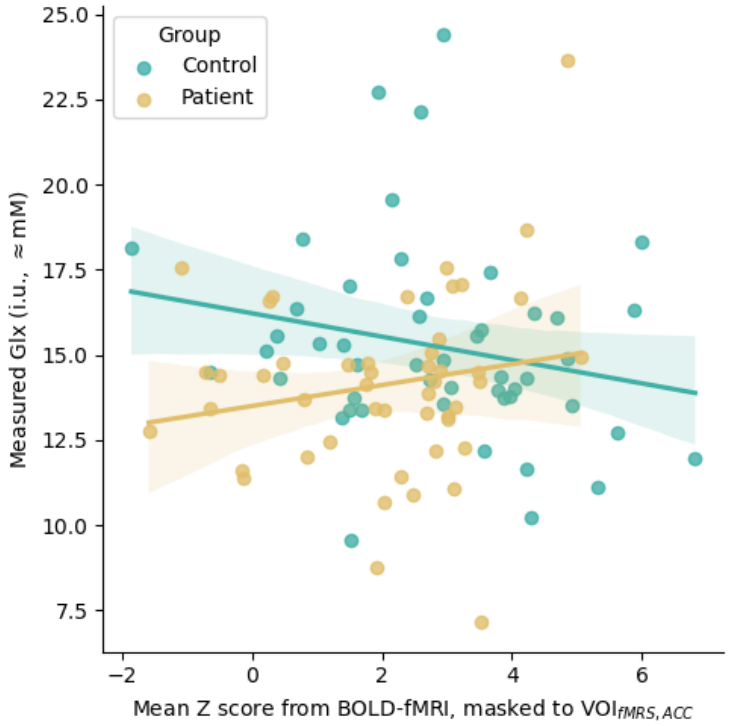

Figure 5 Relation between measured BOLD-fMRI response and measured Glx, showing complementary effects for healthy controls and patients.

No correlation was seen between symptom scores (PANSS P3, total positive, total negative) and baseline metabolite concentration (GABA+ or Glx) or BOLD response (all $p_{holm}>0.05$). Possible associations between behavioural reaction time slowing and total negative symptoms (r=-0.351, $CI_{95\%}$ [-0.578, -0.0747], p=0.0143) and between total positive symptoms and ΔGlx (r=-0.335, $CI_{95\%}$ [-0.57, -0.0496], p=0.0228) did not survive strict correction for multiple comparisons (p_{holm}=0.3, 0.46 respectively) in the present context. Outcomes for all exploratory tests are presented in Supplementary Material, section C.3 (Supplementary Table 5).

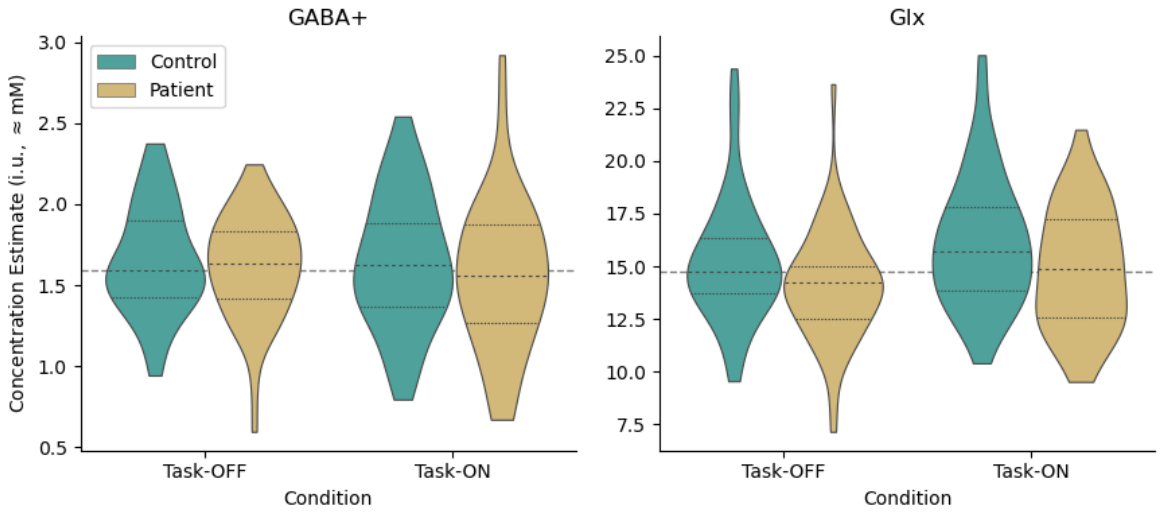

Figure 6 Metabolite estimates by task state and group

Concentration estimates for GABA+ and Glx by group and task condition are presented in Figure 6; additional metabolites estimated from the edit-OFF sub-spectrum (Choline, Creatine, NAA) are presented for interest in Supplementary Figure 2, but not investigated further. Mixed-effects linear modelling showed strong task-related increase in Glx (1.107 i.u., $CI_{95\%}$ [0.343 1.871], $p<0.01$) against an intercept at 13.096 i.u., $CI_{95\%}$ [7.737,18.455], or roughly 8.5% increase in Glx estimate in response to the functional task. The same model indicated reduced baseline Glx in the patient groups (-1.08 i.u., $CI_{95\%}$ [-2.130, -0.030], $p=0.04$), but no evidence of any interaction was found (i.e., no differential effects between task-ON and task-OFF, for patients vs controls ($p>0.5$)). Similar modelling for GABA+ showed no significant effects.

4 Discussion and Conclusions

4.1 Behavioural outcomes

Behavioural outcomes were consistent with expectations based on existing literature[21,51–54], including substantially reduced response accuracy in the patient group indicative of an executive and attentional deficit. However, anticipated prolonged reaction

times[55,56] in the patient group were not significant, likely due to high variance within that group. A previously reported improvement in response accuracy between the fMRS and subsequent fMRI task performance[11], perhaps attributable to learning effects, was also apparent within the current patient group.

4.2 Association with Symptom Scores

Lack of observed correlation between symptom scores (PANSS P3, total positive, total negative) and either the strength of the BOLD response or baseline metabolite concentration may at first seem surprising, especially given previous reports showing such correlations[57–60] (albeit with some contradictory findings[61]). However, we note that high PANSS P3 was a pre-condition for inclusion in the present study, meaning the distribution of symptom scores is not fully representative of the general population of patients with psychosis. Therefore, the absence of correlations in the present study is not necessarily in conflict with existing reports; it may be a result of sensitivity/ceiling effects. Moreover, it may indicate that these factors distinguish low/non-hallucinating subjects from high-hallucinating ones, rather than degrees of severity amongst the higher-hallucinating patients.

4.3 Methodological Considerations

Our previous study on healthy controls showed a significant correlation between the BOLD signal strength assessed by the fMRS and subsequent fMRI acquisition. The moderate degree of this correlation was attributed to inherent variability of each measure, intra-session variability in the BOLD response itself, possible learning effects and/or fatigue. No such correlation could be demonstrated in the patient group of the present study; there are a few possible explanations for this. Within the patient group, BOLD-fMRS measurement showed greater variance than amongst controls – perhaps reflecting reduced reliability of the measurement in the presence of more pronounced subject motion as typically seen amongst

patient groups. BOLD estimates for patients also exhibited a skew towards lower values, particularly evident in the BOLD-fMRS values (Figure 3) and likely reflecting limited conformance amongst some of the participants. Weaker BOLD effects may challenge the sensitivity of the fMRS implementation.

Hence, while the BOLD-fMRS estimates obtained in this way remain useful in certain scenarios (especially where a robust BOLD response is to be expected) and offer the great advantage of temporal concurrency with the MRS acquisition, we would caution against relying solely upon this technique in scenarios where the BOLD response may be more subtle or more variable, or where subject conformance may be limited. Further refinement of the analysis model could potentially improve performance in this regard.

4.4 Baseline Metabolite Concentrations

Our results indicated lower baseline Glx in patients relative to controls in the ACC region. While this is compatible with some previous reports for the region[60–62], recent meta-analyses [63–65] have found differing effects depending on the brain region, and more nuanced associations have been reported in relation to age[66], progression/chronicity[67,68], antipsychotic effects[69] and treatment response[65,70,71]. Studies have also shown correlation between glutamate level and grey matter loss in schizophrenia[72], consistent with neurodegeneration (loss of cortical volume, presumably corresponding with a decrease in glutamatergic synaptic density[73]) and likely associated with age and duration of illness. Inclusion of the fGM factor in our statistical models should limit the impact of this factor on our present findings.

Interpretation of our Glx findings is constrained by a few technical limitations: the meta-analyses suggest different effects for Glu and Gln when assessed separately, with ACC Gln tending to show elevation in patients while ACC Glu exhibits decreases in particular sub-

groups. This may reflect reduced glutamine demand, perhaps as a result of N-methyl-D-aspartic acid (NMDA) receptor hypofunction[74], leading to a net accumulation of glutamine[73]. While no attempt was made to distinguish Glu from Gln in the current dataset, the DIFF spectrum of the TE=68 ms sequence is likely to differ from un-edited, shorter TE sequences in terms of relative sensitivity to each. Inability to distinguish synaptic glutamate from other roles (energy metabolism, protein synthesis etc) may also limit interpretation of these outcomes. Furthermore, our selection criteria target a specific symptom (hallucinatory behaviour) rather than a particular diagnosis. This yields a sample which is heterogeneous with respect to diagnosis, treatment strategy and (presumably) genetic factors; finer-grained analysis considering some of these factors presents an opportunity for further investigation.

We also observe a differential relation between baseline ACC Glx and BOLD-fMRI in the same region: a negative association in healthy controls, contrasting a positive association in patients. This is consistent with the findings of Falkenberg et al [12], and compatible with altered glutamatergic function in schizophrenia[75–78]. Indeed these findings may reflect an underlying neuronal mechanism, with positive association in the patient group perhaps compensatory for overall reduced BOLD activation, with increasing glutamate levels reflecting higher rates of energy turnover in the region [79,80].

4.5 Dynamic Metabolite Concentrations

The finding of increased Glx in response to task (approximately 8.4% increase between task-OFF and task-ON states, across groups) is consistent with our previous study[11] which investigated healthy controls alone, and towards the upper edge of ranges reported in previous meta-analyses (for example, 6.97% $CI_{95\%}$ [5.23, 8.72] change reported by Mullins [81], although typically lower (~3%) for the few studies investigating basic cognitive tasks in the ACC [82–84]). A short-term dynamic change of this magnitude is unlikely to be explained

by metabolic processes alone, but may be consistent with a hypothesized compartmental shift [81,85]. During neural activity, Glu may move from a pool with reduced MRS visibility [86–88] (such as the presynaptic vesicle) to a compartment where it is more visible (such as the cytosol or the synapse), leading to an increase in the MRS-measured signal.

Significantly, the relative task-related change in Glx levels did not differ between healthy controls and patients. Combined with the baseline outcomes, this suggests that existing findings of glutamatergic effects are driven by lower baseline Glx levels in patients, rather than aberrant dynamic regulation in response to task. Furthermore, the absence of observable effects for GABA, either at baseline or as a change in response to task, suggests that neurometabolic effects underlying a putative excitatory/inhibitory imbalance are again driven by baseline Glx deficit, rather than GABAergic abnormalities. Although broadly compatible with the notion of an excitatory-inhibitory imbalance, these findings are less clear in relation to putative NMDA receptor hypofunction[74] and its consequences for GABAergic functions[89]; indeed, it has been proposed that NMDA receptor hypofunction would lead to increased release of synaptic glutamate and underdeveloped GABAergic circuitry.

4.6 Conclusion

In summary: with concurrent measurement of GABA+, Glx and BOLD in response to a cognitive task, we obtained behavioural, functional MR and spectroscopy findings consistent with literature based on separate acquisition of fMRI and MRS, and indicative of an executive and attentional deficit. Limited findings in relation to symptom severity are likely due to limited variation in our defined sample. Reduced baseline Glx in patients, together with a dynamic change comparable with healthy controls in response to task points to tonic rather than phasic effects. Together with an absence of observable differences for GABA this serves to refine our understanding of the roles of these metabolites in a putative

448 Excitatory/Inhibitory imbalance as a possible mechanism underlying the perception of
449 auditory hallucinations.

450

451

5 Author Contributions

ARC: Conceptualization, Methodology, Software, Validation, Formal analysis, Investigation, Data Curation, Writing – Original Draft

GD: Conceptualization, Methodology, Validation, Investigation, Writing – Review & Editing

LE: Methodology, Validation, Resources, Writing – Review & Editing

KK: Data Curation, Writing – Review & Editing

LL: Investigation, Data Curation, Writing – Review & Editing

RN: Methodology, Software, Writing – Review & Editing

LBS: Investigation, Data Curation, Writing – Review & Editing

EJ: Conceptualization, Resources, Writing – Review & Editing, Project administration

KH Conceptualization, Methodology, Resources, Writing – Review & Editing, Supervision, Project administration, Funding acquisition

6 Acknowledgements

This study was funded by the European Research Council (ERC) grant #693124 and by the Western Norway Health Authorities (Helse-Vest) grant #912045 to Kenneth Hugdahl. We are grateful for the radiographers at Haukeland University Hospital: Roger Barndon, Christel Jansen, Turid Randa, Trond Øveraas, Eva Øksnes and Tor Erlend Fjørtoft, for their time and patience with data collection throughout this study.

7 Declaration of interest

Co-authors ARC, LE, KH own shares in NordicNeuroLab (NNL), which produced some of the hardware accessories used during functional MR data acquisition at the scanner. The authors declare no other conflicting interests.

8 Data availability statement

In accordance with data sharing regulations imposed by the Western Norway Ethical Committee (REK-Vest) (https://rekportalen.no/), data may be shared by request to the corresponding author, subject to written permission from the REK-Vest.

Our custom MEGA-PRESS sequence is based on proprietary GE HealthCare code; the authors are in principle willing to share details on our local adaptions through the appropriate vendor-facilitated channels.

Our tools and pipelines for fMRS data modelling are available from: https://git.app.uib.no/bergen-fmri/gaba-temporal-variability

9 References

[1] Hugdahl, K. & Sommer, I. E. Auditory Verbal Hallucinations in Schizophrenia From a Levels of Explanation Perspective. *Schizophr. Bull.* **44**, 234–241 (2018).

[2] Hugdahl, K. Auditory hallucinations: A review of the ERC "VOICE" project. *World J. Psychiatry* **5**, 193 (2015).

[3] Jardri, R. *et al.* Are Hallucinations Due to an Imbalance Between Excitatory and Inhibitory Influences on the Brain? *Schizophr. Bull.* **42**, 1124–1134 (2016).

[4] Ćurčić-Blake, B. *et al.* Interaction of language, auditory and memory brain networks in auditory verbal hallucinations. *Prog. Neurobiol.* **148**, 1–20 (2017).

[5] Craven, A. R. *et al. Linewidth-related bias in modelled concentration estimates from GABA-edited ^{1} H-MRS*. http://biorxiv.org/lookup/doi/10.1101/2024.02.27.582249 (2024) doi:10.1101/2024.02.27.582249.

[6] Hennig, J., Emst, Th., Speck, O., Deuschl, G. & Feifel, E. Detection of brain activation using oxygenation sensitive functional spectroscopy. *Magn. Reson. Med.* **31**, 85–90 (1994).

[7] Zhu, X.-H. & Chen, W. Observed BOLD effects on cerebral metabolite resonances in human visual cortex during visual stimulation: A functional1H MRS study at 4 T. *Magn. Reson. Med.* **46**, 841–847 (2001).

[8] Apšvalka, D., Gadie, A., Clemence, M. & Mullins, P. G. Event-related dynamics of glutamate and BOLD effects measured using functional magnetic resonance spectroscopy (fMRS) at 3 T in a repetition suppression paradigm. *NeuroImage* **118**, 292–300 (2015).

[9] Mescher, M., Merkle, H., Kirsch, J., Garwood, M. & Gruetter, R. Simultaneous in vivo spectral editing and water suppression. *NMR Biomed.* **11**, 266–272 (1998).

[10] Rothman, D. L., Petroff, O. A., Behar, K. L. & Mattson, R. H. Localized 1H NMR measurements of gamma-aminobutyric acid in human brain in vivo. *Proc. Natl. Acad. Sci.* **90**, 5662–5666 (1993).

[11] Craven, A. R. *et al.* GABA, glutamatergic dynamics and BOLD contrast assessed concurrently using functional MRS during a cognitive task. *NMR Biomed.* e5065 (2023) doi:10.1002/nbm.5065.

[12] Falkenberg, L. E. *et al.* Impact of glutamate levels on neuronal response and cognitive abilities in schizophrenia. *NeuroImage Clin.* **4**, 576–584 (2014).

[13] World Health Organization. *The ICD-10 classification of mental and behavioural disorders: clinical descriptions and diagnostic guidelines*. (World Health Organization, 1992).

[14] World Health Organization. *ICD-10 psykiske lidelser og atferdsforstyrrelser: kliniske beskrivelser og diagnostiske retningslinjer*. (Universitetsforlaget, 2016).

[15] Kay, S. R., Fiszbein, A. & Opler, L. A. The Positive and Negative Syndrome Scale (PANSS) for Schizophrenia. *Schizophr. Bull.* **13**, 261–276 (1987).

[16] Chadwick, P., Lees, S. & Birchwood, M. The revised Beliefs About Voices Questionnaire (BAVQ–R). *Br. J. Psychiatry* **177**, 229–232 (2000).

[17] Hugdahl, K. *et al.* The phenomenology of auditory verbal hallucinations in schizophrenia assessed with the MiniVoiceQuestionnaire (MVQ). Preprint at https://doi.org/10.1101/2023.02.16.23285636 (2023).

[18] WHO Collaborating Centre for Drug Statistics Methodology. *ATC classification index with DDDs, 2024*. (WHO Collaborating Centre for Drug Statistics Methodology, Oslo, Norway, 2024).

[19] Lin, A. *et al.* Minimum Reporting Standards for in vivo Magnetic Resonance Spectroscopy (MRSinMRS): Experts' consensus recommendations. *NMR Biomed.* (2021) doi:10.1002/nbm.4484.

[20] Eriksen, B. A. & Eriksen, C. W. Effects of noise letters upon the identification of a target letter in a nonsearch task. *Percept. Psychophys.* **16**, 143–149 (1974).

[21] Kopp, B., Mattler, U. & Rist, F. Selective attention and response competition in schizophrenic patients. *Psychiatry Res.* **53**, 129–139 (1994).

[22] Lally, N. *et al.* Glutamatergic correlates of gamma-band oscillatory activity during cognition: A concurrent ER-MRS and EEG study. *NeuroImage* **85**, 823–833 (2014).

[23] Edden, R. A. E., Puts, N. A. J., Harris, A. D., Barker, P. B. & Evans, C. J. Gannet: A batch-processing tool for the quantitative analysis of gamma-aminobutyric acid-edited MR spectroscopy spectra: Gannet: GABA Analysis Toolkit. *J. Magn. Reson. Imaging* **40**, 1445–1452 (2014).

[24] Near, J. *et al.* Frequency and phase drift correction of magnetic resonance spectroscopy data by spectral registration in the time domain: MRS Drift Correction Using Spectral Registration. *Magn. Reson. Med.* **73**, 44–50 (2015).

[25] Mikkelsen, M. *et al.* Correcting frequency and phase offsets in MRS data using robust spectral registration. *NMR Biomed.* **33**, (2020).

[26] Craven, A. R., Ersland, L., Hugdahl, K. & Gruner, R. *Modelling inter-shot variability for robust temporal sub-sampling of dynamic, GABA-edited MR spectroscopy data*. http://biorxiv.org/lookup/doi/10.1101/2024.12.05.627018 (2024) doi:10.1101/2024.12.05.627018.

[27] Bartha, R., Drost, D. J., Menon, R. S. & Williamson, P. C. Spectroscopic lineshape correction by QUECC: Combined QUALITY deconvolution and eddy current correction. *Magn. Reson. Med.* **44**, 641–645 (2000).

[28] Metz, K. R., Lam, M. M. & Webb, A. G. Reference deconvolution: A simple and effective method for resolution enhancement in nuclear magnetic resonance spectroscopy. *Concepts Magn. Reson.* **12**, 21–42 (2000).

[29] Maudsley, A. A. Spectral Lineshape Determination by Self-Deconvolution. *J. Magn. Reson. B* **106**, 47–57 (1995).

[30] Jenkinson, M., Bannister, P., Brady, M. & Smith, S. Improved Optimization for the Robust and Accurate Linear Registration and Motion Correction of Brain Images. *NeuroImage* **17**, 825–841 (2002).

[31] Smith, S. M. Fast robust automated brain extraction. *Hum. Brain Mapp.* **17**, 143–155 (2002).

[32] Jenkinson, M. & Smith, S. A global optimisation method for robust affine registration of brain images. *Med. Image Anal.* **5**, 143–156 (2001).

[33] Andersson, J. L., Jenkinson, M. & Smith, S. Non-linear optimisation FMRIB technical report TR07JA1. *Practice* (2007).

[34] Andersson, J. L., Jenkinson, M., Smith, S., & others. Non-linear registration, aka Spatial normalisation FMRIB technical report TR07JA2. *FMRIB Anal. Group Univ. Oxf.* **2**, e21 (2007).

[35] Grabner, G. *et al.* Symmetric Atlasing and Model Based Segmentation: An Application to the Hippocampus in Older Adults. in *Medical Image Computing and Computer-Assisted Intervention – MICCAI 2006* (eds. Larsen, R., Nielsen, M. & Sporring, J.) vol. 4191 58–66 (Springer Berlin Heidelberg, 2006).

[36] Woolrich, M. W., Ripley, B. D., Brady, M. & Smith, S. M. Temporal Autocorrelation in Univariate Linear Modeling of FMRI Data. *NeuroImage* **14**, 1370–1386 (2001).

[37] Worsley, K. J. Statistical analysis of activation images. Ch 14. in *Functional MRI: An introduction to methods* (eds. Jezzard, P., Matthews, P. M. & Smith, S. M.) 251–270 (2001).

[38] Pernet, C., Wilcox, R. & Rousselet, G. Robust Correlation Analyses: False Positive and Power Validation Using a New Open Source Matlab Toolbox. *Front. Psychol.* **3**, (2013).

[39] Rousselet, G. A. & Pernet, C. R. Improving standards in brain-behavior correlation analyses. *Front. Hum. Neurosci.* **6**, (2012).

[40] Belsley, D. A., Kuh, E. & Welsch, R. E. *Regression diagnostics: identifying influential data and sources of collinearity*. (Wiley, 1980).

[41] Jarque, C. M. & Bera, A. K. A Test for Normality of Observations and Regression Residuals. *Int. Stat. Rev. Rev. Int. Stat.* **55**, 163 (1987).

[42] White, H. A Heteroskedasticity-Consistent Covariance Matrix Estimator and a Direct Test for Heteroskedasticity. *Econometrica* **48**, 817 (1980).

[43] Seabold, S. & Perktold, J. statsmodels: Econometric and statistical modeling with python. in (2010).

[44] Vallat, R. Pingouin: statistics in Python. *J. Open Source Softw.* **3**, 1026 (2018).

[45] SciPy 1.0 Contributors *et al.* SciPy 1.0: fundamental algorithms for scientific computing in Python. *Nat. Methods* **17**, 261–272 (2020).

[46] McKinney, W. Data Structures for Statistical Computing in Python. in (eds. van der Walt, S. & Millman, J.) 56–61 (2010). doi:10.25080/Majora-92bf1922-00a.

[47] Harris, C. R. *et al.* Array programming with NumPy. *Nature* **585**, 357–362 (2020).

[48] Hunter, J. D. Matplotlib: A 2D Graphics Environment. *Comput. Sci. Eng.* **9**, 90–95 (2007).

[49] Waskom, M. seaborn: statistical data visualization. *J. Open Source Softw.* **6**, 3021 (2021).

[50] Charlier, F. *et al.* trevismd/statannotations: v0.5. (2022) doi:10.5281/ZENODO.7213391.

[51] Davelaar, E. J. & Stevens, J. Sequential dependencies in the Eriksen flanker task: A direct comparison of two competing accounts. *Psychon. Bull. Rev.* **16**, 121–126 (2009).

[52] Ridderinkhof, K. R., Wylie, S. A., van den Wildenberg, W. P. M., Bashore, T. R. & van der Molen, M. W. The arrow of time: Advancing insights into action control from the arrow version of the Eriksen flanker task. *Atten. Percept. Psychophys.* **83**, 700–721 (2021).

[53] Stoffels, E. J. & van der Molen, M. W. Effects of visual and auditory noise on visual choice reaction time in a continuous-flow paradigm. *Percept. Psychophys.* **44**, 7–14 (1988).

[54] Ettinger, U. *et al.* Response inhibition and interference control: Effects of schizophrenia, genetic risk, and schizotypy. *J. Neuropsychol.* **12**, 484–510 (2018).

[55] Yücel, M. *et al.* Impairments of response conflict monitoring and resolution in schizophrenia. *Psychol. Med.* **32**, 1251–1260 (2002).

[56] Gooding, D. C., Braun, J. G. & Studer, J. A. Attentional network task performance in patients with schizophrenia–spectrum disorders: Evidence of a specific deficit. *Schizophr. Res.* **88**, 169–178 (2006).

[57] Hjelmervik, H. *et al.* Intra-Regional Glu-GABA vs Inter-Regional Glu-Glu Imbalance: A 1H-MRS Study of the Neurochemistry of Auditory Verbal Hallucinations in Schizophrenia. *Schizophr. Bull.* **46**, 633–642 (2020).

[58] Hjelmervik, H. *et al.* Negative valence of hallucinatory voices as predictor of cortical glutamatergic metabolite levels in schizophrenia patients. *Brain Behav.* **12**, (2022).

[59] Li, J. *et al.* Anterior Cingulate Cortex Glutamate Levels Are Related to Response to Initial Antipsychotic Treatment in Drug-Naive First-Episode Schizophrenia Patients. *Front. Psychiatry* **11**, 553269 (2020).

[60] Hugdahl, K. *et al.* Glutamate as a mediating transmitter for auditory hallucinations in schizophrenia: A 1H MRS study. *Schizophr. Res.* **161**, 252–260 (2015).

[61] Ćurčić-Blake, B. *et al.* Glutamate in dorsolateral prefrontal cortex and auditory verbal hallucinations in patients with schizophrenia: A 1 H MRS study. *Prog. Neuropsychopharmacol. Biol. Psychiatry* **78**, 132–139 (2017).

[62] Singh, S. *et al.* Evidence for regional hippocampal damage in patients with schizophrenia. *Neuroradiology* **60**, 199–205 (2018).

[63] Merritt, K. *et al.* Variability and magnitude of brain glutamate levels in schizophrenia: a meta and mega-analysis. *Mol. Psychiatry* **28**, 2039–2048 (2023).

[64] Merritt, K., Egerton, A., Kempton, M. J., Taylor, M. J. & McGuire, P. K. Nature of Glutamate Alterations in Schizophrenia: A Meta-analysis of Proton Magnetic Resonance Spectroscopy Studies. *JAMA Psychiatry* **73**, 665 (2016).

[65] Nakahara, T. *et al.* Glutamatergic and GABAergic metabolite levels in schizophrenia-spectrum disorders: a meta-analysis of 1H-magnetic resonance spectroscopy studies. *Mol. Psychiatry* **27**, 744–757 (2022).

[66] Brandt, A. S. *et al.* Age-related changes in anterior cingulate cortex glutamate in schizophrenia: A 1H MRS Study at 7Tesla. *Schizophr. Res.* **172**, 101–105 (2016).

[67] Liemburg, E. *et al.* Prefrontal NAA and Glx Levels in Different Stages of Psychotic Disorders: a 3T 1H-MRS Study. *Sci. Rep.* **6**, 21873 (2016).

[68] Ohrmann, P. *et al.* Cognitive impairment and in vivo metabolites in first-episode neuroleptic-naive and chronic medicated schizophrenic patients: A proton magnetic resonance spectroscopy study. *J. Psychiatr. Res.* **41**, 625–634 (2007).

[69] Kubota, M., Moriguchi, S., Takahata, K., Nakajima, S. & Horita, N. Treatment effects on neurometabolite levels in schizophrenia: A systematic review and meta-analysis of proton magnetic resonance spectroscopy studies. *Schizophr. Res.* **222**, 122–132 (2020).

[70] Mouchlianitis, E. *et al.* Treatment-Resistant Schizophrenia Patients Show Elevated Anterior Cingulate Cortex Glutamate Compared to Treatment-Responsive. *Schizophr. Bull.* **42**, 744–752 (2016).

[71] Egerton, A. *et al.* Response to initial antipsychotic treatment in first episode psychosis is related to anterior cingulate glutamate levels: a multicentre 1H-MRS study (OPTiMiSE). *Mol. Psychiatry* **23**, 2145–2155 (2018).

[72] Aoyama, N. *et al.* Grey matter and social functioning correlates of glutamatergic metabolite loss in schizophrenia. *Br. J. Psychiatry* **198**, 448–456 (2011).

[73] Coyle, J. T. & Konopaske, G. Glutamatergic Dysfunction in Schizophrenia Evaluated With Magnetic Resonance Spectroscopy. *JAMA Psychiatry* **73**, 649 (2016).

[74] Coyle, J. T. Glutamate and Schizophrenia: Beyond the Dopamine Hypothesis. *Cell. Mol. Neurobiol.* **26**, 363–382 (2006).

[75] Dwyer, G. E., Hugdahl, K., Specht, K. & Grüner, R. Current Practice and New Developments in the Use of In Vivo Magnetic Resonance Spectroscopy for the Assessment of Key Metabolites Implicated in the Pathophysiology of Schizophrenia. *Curr. Top. Med. Chem.* **18**, 1908–1924 (2019).

[76] Duarte, J. M. N. & Xin, L. Magnetic Resonance Spectroscopy in Schizophrenia: Evidence for Glutamatergic Dysfunction and Impaired Energy Metabolism. *Neurochem. Res.* **44**, 102–116 (2019).

[77] Benes, F. M., Sorensen, I., Vincent, S. L., Bird, E. D. & Sathi, M. Increased Density of Glutamate-immunoreactive Vertical Processes in Superficial Laminae in Cingulate Cortex of Schizophrenic Brain. *Cereb. Cortex* **2**, 503–512 (1992).

[78] Woo, T.-U. W., Shrestha, K., Lamb, D., Minns, M. M. & Benes, F. M. N-Methyl-D-Aspartate Receptor and Calbindin-Containing Neurons in the Anterior Cingulate Cortex in Schizophrenia and Bipolar Disorder. *Biol. Psychiatry* **64**, 803–809 (2008).

[79] Mangia, S. *et al.* Sustained Neuronal Activation Raises Oxidative Metabolism to a New Steady-State Level: Evidence from ^{1}H NMR Spectroscopy in the Human Visual Cortex. *J. Cereb. Blood Flow Metab.* **27**, 1055–1063 (2007).

[80] Rothman, D. L., Behar, K. L., Hyder, F. & Shulman, R. G. In vivo NMR Studies of the Glutamate Neurotransmitter Flux and Neuroenergetics: Implications for Brain Function. *Annu. Rev. Physiol.* **65**, 401–427 (2003).

[81] Mullins, P. G. Towards a theory of functional magnetic resonance spectroscopy (fMRS): A meta-analysis and discussion of using MRS to measure changes in neurotransmitters in real time. *Scand. J. Psychol.* **59**, 91–103 (2018).

[82] Kühn, S. *et al.* Neurotransmitter changes during interference task in anterior cingulate cortex: evidence from fMRI-guided functional MRS at 3 T. *Brain Struct. Funct.* **221**, 2541–2551 (2016).

[83] Taylor, R. *et al.* Increased glutamate levels observed upon functional activation in the anterior cingulate cortex using the Stroop Task and functional spectroscopy. *NeuroReport* **26**, 107–112 (2015).

[84] Taylor, R. *et al.* Functional magnetic resonance spectroscopy of glutamate in schizophrenia and major depressive disorder: anterior cingulate activity during a color-word Stroop task. *Npj Schizophr.* **1**, 15028 (2015).

[85] Lea-Carnall, C. A., El-Deredy, W., Stagg, C. J., Williams, S. R. & Trujillo-Barreto, N. J. A mean-field model of glutamate and GABA synaptic dynamics for functional MRS. *NeuroImage* **266**, 119813 (2023).

[86] Kauppinen, R. A., Pirttilä, T. R. M., Auriola, S. O. K. & Williams, S. R. Compartmentation of cerebral glutamate *in situ* as detected by 1H/13C n.m.r. *Biochem. J.* **298**, 121–127 (1994).

[87] Rae, C. *et al.* Inhibition of glutamine transport depletes glutamate and GABA neurotransmitter pools: further evidence for metabolic compartmentation: Role of glutamine transport in CNS metabolism. *J. Neurochem.* **85**, 503–514 (2003).

[88] Hancu, I. & Port, J. The case of the missing glutamine. *NMR Biomed.* **24**, 529–535 (2011).

[89] Cohen, S. M., Tsien, R. W., Goff, D. C. & Halassa, M. M. The impact of NMDA receptor hypofunction on GABAergic neurons in the pathophysiology of schizophrenia. *Schizophr. Res.* **167**, 98–107 (2015).

10 Figure Captions

A Additional Subject Details

	n	ICD-10	Diagnosis
Schizophrenia	**29**		
	23	F20.0	Paranoid schizophrenia
	3	F20.3	Undifferentiated schizophrenia
	1	F20.4	Post-schizophrenic depression
	2	F20.9	Schizophrenia, unspecified
Other Schiz. Spectrum	**7**		
	1	F23.3	Acute paranoid psychosis
	2	F25.0	Schizoaffective disorder, manic type
	1	F25.1	Schizoaffective disorder, depressive type
	3	F29	Unspecified non-organic psychosis
Mood/affective	**2**		
	1	F31	Bipolar disorder
	1	F32.3	Severe depressive episode with psychotic symptoms
Personality/behavioural	**4**		
	1	F60.0	Paranoid personality disorder
	1	F60.3	Emotionally unstable personality disorder
	1	F61.0	Mixed and other personality disorders
	1	F62.8	Other enduring personality changes
Drug-induced psychosis	**4**		Mental and behavioural disorders due to…
	1	F12.5	Use of cannabinoids; psychotic disorder
	2	F19.0	Multiple drug use and use of other psychoactive substances; acute intoxication
	1	F19.52	…psychosis, mainly with hallucinations
Other	**5**		
	1	F06.0	Organic hallucinosis
	1	F90	Disturbance of activity and attention
	2	N/A	Unknown diagnosis
	1	N/A	No diagnosis

Supplementary Table 1 Diagnoses of patients in the present study, according to ICD-10 criteria

Diagnoses are according to the ICD-10 criteria, described in the following publications (English and Norwegian translation):

World Health Organization. (1992). *The ICD-10 classification of mental and behavioural disorders: Clinical descriptions and diagnostic guidelines* (Reprinted). World Health Organization. https://www.who.int/docs/default-source/classification/other-classifications/bluebook.pdf

World Health Organization. (2016). *ICD-10 psykiske lidelser og atferdsforstyrrelser: Kliniske beskrivelser og diagnostiske retningslinjer* (10. rev., 19. oppl). Universitetsforlaget. https://www.ehelse.no/kodeverk-og-terminologi/ICD-10-og-ICD-11

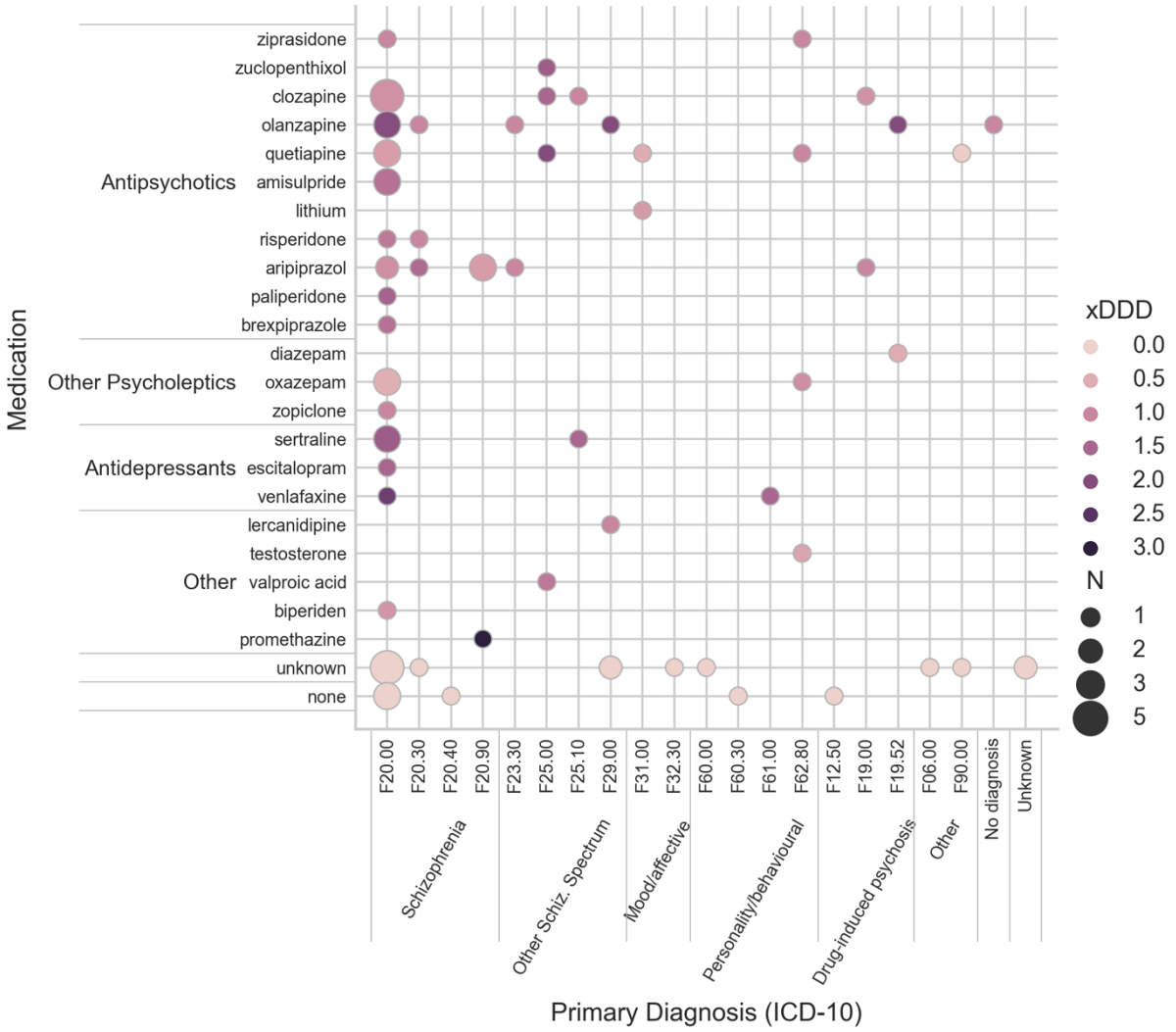

Supplementary Figure 1 Medication and mean of the (maximum) prescribed dosage, expressed relative to the defined daily dose (DDD). Size of the points is proportional to the number of patients (N), with darker shading indicating higher dosage (xDDD).

In several cases, the prescribed dosage was qualified with terms such as “up to” and “as needed” (“opp til”, “ved behov”); some subjects reported that they had not taken prescribed medicine in the period leading up to the study. Dosage presented here therefore represents the maximum prescribed dosage, and is likely to slightly overestimate the actual dosage taken.

Defined daily dose (DDD) according to WHO Collaborating Centre for Drug Statistics Methodology, ATC classification index with DDDs, 2024. Oslo, Norway 2024, searchable online at https://atcddd.fhi.no/atc_ddd_index/

ATC codes were derived from trade names via the register at https://www.felleskatalogen.no/medisin/atc-register/

B MRSinMRS checklist

Site (name or number)	Haukeland University Hospital
1. Hardware	
a. Field strength [T]	3 T
b. Manufacturer	GE HealthCare
c. Model (software version if available)	MR 750, DV 28
d. RF coils: nuclei (transmit/receive), number of channels, type, body part	GEHC 8-channel ^{1}H head coil
e. Additional hardware	NNL visual system, response grips and SyncBox for functional task
2. Acquisition	
a. Pulse sequence	MEGA-PRESS (GABA+ editing, ATSM patch), adapted for triggering and with additional water-unsuppressed reference scans (every third FID)
b. Volume of interest (VOI) locations	Anterior Cingulate Cortex
c. Nominal VOI size [cm3,mm3]	22 x 36 x 23 mm^3 (18.2 mL)
d. Repetition time (T_R), echo time (T_E) [ms, s]	T_R = 1500 ms, T_E = 68 ms
e. Total number of excitations or acquisitions per spectrum In time series for kinetic studies i. Number of averaged spectra (NA) per time point ii. Averaging method (eg block-wise or moving average) iii. Total number of spectra (acquired/in time series)	700 transients, alternating edit-ON/-OFF with CHESS suppression pulses disabled in every third transient averages. Of these, 220 were preceded by task stimulus (grouped into 30-second task-ON blocks, separated by 60-second task-OFF blocks) Further subdivided into even time bins (roughly 73 averages each), and according to stimulus and response (varying sizes)
f. Additional sequence parameters (spectral width in Hz, number of spectral points, frequency offsets) If STEAM:, mixing time (T_M) If MRSI: 2D or 3D, FOV in all directions, matrix size, acceleration factors, sampling method	Spectral width 5000Hz, 4096 data points 15 ms editing pulses at 1.9 ppm (edit-ON) and 7.46 ppm (edit-OFF)
g. Water suppression method	CHESS
h. Shimming method, reference peak, and thresholds for "acceptance of shim" chosen	Vendor default prescan (double-echo GRE)
i. Triggering or motion correction method (respiratory, peripheral, cardiac triggering, incl. device used and delays)	MRS served as trigger source for the functional paradigm
3. Data analysis methods and outputs	
a. Analysis software	Gannet 3.1, with in-house methods to extract functional subsets between GannetLoad and GannetFit modules.
b. Processing steps deviating from quoted reference or product	Spectra extracted from decomposition of full set of transients, described in section 2.2
c. Output measure (eg absolute concentration, institutional units, ratio), processing steps deviating from quoted reference or product	Water-referenced estimates for GABA+ and Glx, with adjustment for voxel tissue content
d. Quantification references and assumptions, fitting model assumptions	N/A
4. Data quality	
a. Reported variables (SNR, linewidth (with reference peaks))	SNR NAA: 97.7±11.1/95.7±12.9; 41.9±3.95/40.8±3.79 FWHM NAA (Hz): 6.91±0.73/6.97±0.73; 7.22±0.61/7.27±0.76 FWHM GABA+ (Hz): 18±1.82/16±2.5; 18.8±1.59/16.8±2.69 Denoted median±MAD, patient/control, task-OFF; task-ON
b. Data exclusion criteria	FWHM linewidth > 12 Hz (NAA_{diff}) or > 30 Hz ($GABA+_{diff}$) SNR extraordinarily low, < 20 (NAA_{diff}) Extreme outliers (> 5 x median absolute deviation) for $GABA+_{diff}$ or Glx_{diff} estimate; See section 2.2
c. Quality measures of postprocessing model fitting (eg CRLB, goodness of fit, SD of residual)	Strong outlier removal and robust statistics only: individual fits to event-related data expected to be of lower quality than non-functional MRS.
d. Sample spectrum	See Figure 4

Supplementary Table 2 MRSinMRS checklist[19] summarising key details of the MRS acquisition

C Supplementary Results

Session	Group	N subjects	Stimulus Type	N stimuli (per subj.)	Achieved ISI mean (ms)	Achieved ISI SD (ms)	RT (ms)	RA (% correct)	RA/RT
fMRS	Control	51	Congruent	132	1499.6 ± 5.6	107.3 ± 6.8	428.7 ± 38.9 ***/n.s./n.s.	98.5 ± 3.5 ***/n.s./***	.228 ± .022 ***/n.s./***
			Incongruent	88	1504.5 ± 8.7	108.2 ± 5.1	522.2 ± 51.0 ***/n.s./n.s.	84.1 ± 14.8 ***/***/***	.159 ± .029 ***/***/***
			Difference		(incompatibility slowing)		92.7 ± 23.3 ***/n.s./n.s.		
	Patient	51	Congruent	132	1501.7 ± 7.0	107.0 ± 10.4	451.6 ± 77.8 ***/n.s./n.s.	86.4 ± 18.7 ***/n.s./***	.182 ± .044 ***/n.s./***
			Incongruent	88	1500.9 ± 10.7	106.0 ± 12.9	538.0 ± 113.0 ***/n.s./n.s.	54.5 ± 23.8 ***/***/***	.100 ± .041 ***/***/***
			Difference		(incompatibility slowing)		103.8 ± 51.0 ***/n.s./n.s.		
fMRI	Control	51	Congruent	72	1496.9 ± 7.5	102.8 ± 6.1	437.3 ± 39.0 ***/n.s./n.s.	98.6 ± 3.1 ***/n.s./***	.225 ± .021 ***/n.s./***
			Incongruent	48	1503.0 ± 11.0	102.7 ± 7.1	520.5 ± 49.4 ***/n.s./n.s.	89.6 ± 13.7 ***/***/***	.161 ± .025 ***/***/***
			Difference		(incompatibility slowing)		84.7 ± 21.0 ***/n.s./n.s.		
	Patient	49	Congruent	72	1498.5 ± 7.1	101.6 ± 6.2	454.7 ± 72.6 ***/n.s./n.s.	93.1 ± 17.3 ***/n.s./***	.193 ± .039 ***/n.s./***
			Incongruent	48	1501.3 ± 9.3	103.4 ± 8.0	561.0 ± 91.6 ***/n.s./n.s.	64.6 ± 24.1 ***/***/***	.119 ± .038 ***/***/***
			Difference		(incompatibility slowing)		90.7 ± 41.8 ***/n.s./n.s.		

*Supplementary Table 3 Behavioural outcomes from the Flanker task; values are quoted as Median +/- Median Absolute Deviation (MAD) of per-subject outcomes. Significant differences are indicated between stimulus type, session and group (denoted type/session/group, *** $p_{holm}<0.001$, ** $p_{holm}<0.01$, * $p_{holm}<0.05$, n.s. not significant). ISI: Inter-stimulus interval, RA: Response Accuracy, RT: Response Time*

	Control		Patient	
	task-OFF	task-ON	task-OFF	task-ON
SNR NAA	97.7 ± 11.1	41.9 ± 3.95	95.7 ± 12.9	40.8 ± 3.79
FWHM Cho/Cr *before* linewidth matching n.s.	6.84 ± 0.569	6.72 ± 0.619	7.07 ± 0.474	7.02 ± 0.518
FWHM Cho/Cr *after* linewidth matching n.s.	6.88 ± 0.569	7.03 ± 0.651	7.24 ± 0.54	7.23 ± 0.509
FWHM NAA (Hz)	6.91 ± 0.729	6.97 ± 0.729	7.22 ± 0.608	7.27 ± 0.764
FWHM GABA+ (Hz)	18 ± 1.82	16.3 ± 2.5	18.8 ± 1.59	16.8 ± 2.69
FWHM Glx (Hz)	12.1 ± 1.11	12.7 ± 1.47	12.3 ± 0.9	12.5 ± 1.49
GABA+ (i.u., ≈mM)	2.9 ± 0.367	2.88 ± 0.46	2.87 ± 0.372	2.79 ± 0.594
Glx (i.u., ≈mM)	14.7 ± 1.35	15.7 ± 2.03	14.2 ± 1.33	14.9 ± 2.39

Supplementary Table 4 Quality metrics and concentration estimates from the fMRS analysis, task-ON vs task-OFF, presented as median ± MAD.

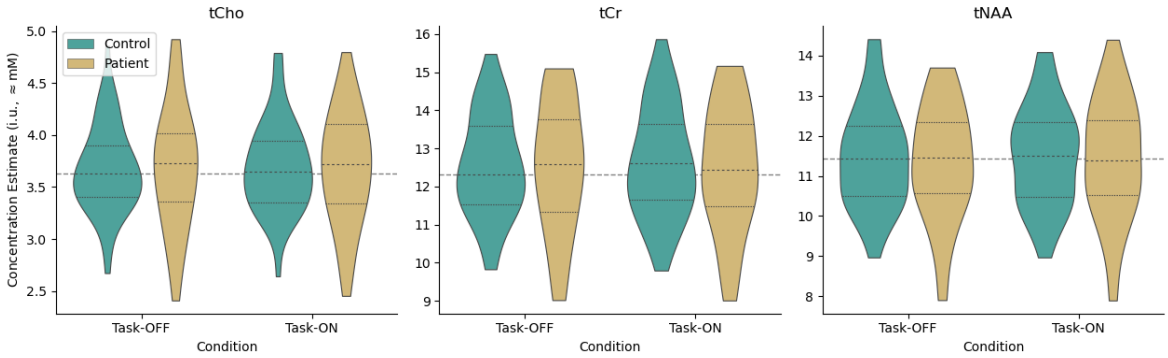

Supplementary Figure 2 Concentration estimates for other metabolites according to group and condition (obtained from the edit-OFF sub-spectrum using the Gannet peak-fitting model)

C.1 Regression Modelling Outcomes: Glx

Associations between baseline Glx estimate, BOLD signal strength and interactions with patient and control groups, with voxel grey matter fraction fGM as a covariate (ie, `Glx ~ C(group)*BOLD + fGM`), after removing outlier observations:

OLS Regression Results

Dep. Variable:	Glx_ConcIU_rest	R-squared:	0.152
Model:	OLS	Adj. R-squared:	0.110
Method:	Least Squares	F-statistic:	3.627
Date:	Mon, 14 Oct 2024	Prob (F-statistic):	0.00905
Time:	15:26:06	Log-Likelihood:	-167.59
No. Observations:	86	AIC:	345.2
Df Residuals:	81	BIC:	357.5
Df Model:	4		
Covariance Type:	nonrobust		

	coef	std err	t	P>|t|	[0.025	0.975]
Intercept	14.7549	2.389	6.176	0.000	10.001	19.509
C(group, Treatment("control"))[T.patient]	**-2.3603**	**0.663**	**-3.557**	**0.001**	**-3.680**	**-1.040**
BOLD	**-0.3937**	**0.147**	**-2.681**	**0.009**	**-0.686**	**-0.102**
C(group, Treatment("control"))[T.patient]:BOLD	**0.5860**	**0.238**	**2.463**	**0.016**	**0.113**	**1.059**
fGM	2.0133	3.787	0.532	0.596	-5.523	9.549

Omnibus:	1.838	Durbin-Watson:	2.120
Prob(Omnibus):	0.399	Jarque-Bera (JB):	1.795
Skew:	0.275	Prob(JB):	0.408
Kurtosis:	2.553	Cond. No.	78.1

Glx estimate in relation to group (patient, control), task status (task-OFF, task-ON), with grey matter fraction as a covariate and subject as the grouping variable (ie, `Glx ~ C(group)*C(task_state) + fGM`), after filtering observations with strong residuals:

Mixed Linear Model Regression Results

Model:	MixedLM	Dependent Variable:	value
No. Observations:	193	Method:	REML
No. Groups:	99	Scale:	3.5542
Min. group size:	1	Log-Likelihood:	-442.9158
Max. group size:	2	Converged:	Yes
Mean group size:	1.9		

	Coef.	Std.Err.	z	P>|z|	[0.025	0.975]
Intercept	13.096	2.734	4.790	0.000	7.737	18.455
C(task_state)[T.True]	**1.107**	**0.390**	**2.840**	**0.005**	**0.343**	**1.871**
C(group, Treatment("control"))[T.patient]	**-1.080**	**0.536**	**-2.017**	**0.044**	**-2.130**	**-0.030**
C(task_state)[T.True]:C(group, Treatment("control"))[T.pat	-0.106	0.546	-0.194	0.846	-1.177	0.965
fGM	3.030	4.492	0.675	0.500	-5.773	11.834
subject Var	3.315	0.574				

C.2 Regression Modelling Outcomes: GABA+

Associations between baseline GABA+ estimate, BOLD signal strength and interactions with patient and control groups, with voxel grey matter fraction fGM as a covariate (ie, `GABA ~ C(group)*BOLD + fGM`), after removing outlier observations:

OLS Regression Results

Dep. Variable:	GABA_rest	R-squared:	0.073
Model:	OLS	Adj. R-squared:	0.029
Method:	Least Squares	F-statistic:	1.649
Date:	Mon, 14 Oct 2024	Prob (F-statistic):	0.170
Time:	15:26:00	Log-Likelihood:	-10.491
No. Observations:	89	AIC:	30.98
Df Residuals:	84	BIC:	43.43
Df Model:	4		
Covariance Type:	nonrobust		

	coef	std err	t	P>|t|	[0.025	0.975]
Intercept	1.7804	0.384	4.639	0.000	1.017	2.544
C(group, Treatment("control"))[T.patient]	-0.2491	0.108	-2.297	0.024	-0.465	-0.033
BOLD	-0.0577	0.025	-2.280	0.025	-0.108	-0.007
C(group, Treatment("control"))[T.patient]:BOLD	0.0870	0.038	2.264	0.026	0.011	0.163
fGM	0.0252	0.607	0.041	0.967	-1.181	1.231

Omnibus:	0.113	Durbin-Watson:	2.258
Prob(Omnibus):	0.945	Jarque-Bera (JB):	0.284
Skew:	0.047	Prob(JB):	0.868
Kurtosis:	2.740	Cond. No.	79.5

GABA+ estimate in relation to group (patient, control), task status (task-OFF, task-ON), with grey matter fraction as a covariate and subject as the grouping variable (ie, `GABA ~ C(group)*C(task_state) + fGM`), after filtering observations with strong residuals:

Mixed Linear Model Regression Results

Model:	MixedLM	Dependent Variable:	value
No. Observations:	192	Method:	REML
No. Groups:	99	Scale:	0.0612
Min. group size:	1	Log-Likelihood:	-64.0653
Max. group size:	2	Converged:	Yes
Mean group size:	1.9		

	Coef.	Std.Err.	z	P>|z|	[0.025	0.975]
Intercept	1.426	0.368	3.873	0.000	0.704	2.147
C(task_state)[T.True]	0.008	0.050	0.165	0.869	-0.090	0.107
C(group, Treatment("control"))[T.patient]	-0.019	0.071	-0.271	0.787	-0.159	0.120
C(task_state)[T.True]:C(group, Treatment("control"))[T.pat	-0.065	0.072	-0.896	0.370	-0.206	0.077
fGM	0.348	0.606	0.574	0.566	-0.840	1.535
subject Var	0.063	0.078				

C.3 Exploratory correlational tests

Variables ®	PANSS P3			PANSS total positive			PANSS total negative		
-	r	$p_{unc.}$	p_{holm}	r	$p_{unc.}$	p_{holm}	r	$p_{unc.}$	p_{holm}
Baseline Glx	-0.00 [-0.29, 0.28]	0.974	1	0.01 [-0.28, 0.29]	0.963	1	-0.06 [-0.34, 0.22]	0.661	1
ΔGlx	-0.01 [-0.29, 0.27]	0.945	1	**-0.34 [-0.57,-0.05]**	**0.0228**	**0.457**	-0.01 [-0.29, 0.27]	0.96	1
Baseline GABA+	-0.17 [-0.45, 0.15]	0.293	1	-0.14 [-0.41, 0.15]	0.337	1	0.05 [-0.24, 0.32]	0.744	1
ΔGABA+	-0.15 [-0.41, 0.14]	0.312	1	-0.03 [-0.32, 0.27]	0.858	1	0.07 [-0.22, 0.35]	0.618	1
BOLD-fMRI	-0.08 [-0.38, 0.23]	0.598	1	-0.10 [-0.38, 0.20]	0.508	1	-0.11 [-0.39, 0.18]	0.458	1
Task performance: RA/RT	-0.19 [-0.47, 0.13]	0.241	1	-0.15 [-0.42, 0.14]	0.301	1	-0.28 [-0.52, 0.00]	0.0536	1
Task performance: RT_slowing	-0.24 [-0.49, 0.05]	0.0982	1	-0.24 [-0.49, 0.05]	0.0988	1	**-0.35 [-0.58,-0.07]**	**0.0143**	**0.301**

Supplementary Table 5 Exploratory correlational testing; skipped Spearman correlation with 95% confidence interval